Cell-Encapsulating Hydrogel Puzzle: Polyrotaxane-Based Self-Healing Hydrogels

Cho, Ik Sung

Ooya, Tooru

(Citation)
Chemistry-A European Journal,26(4):913-920

(Issue Date)
2020-01-16

(Resource Type)
journal article

(Version)
Accepted Manuscript

Cell-Encapsulating Hydrogel Puzzle: Polyrotaxane-Based Self-Healing Hydrogels

Ik Sung Cho,[a] and Tooru Ooya*[a]

Abstract: Slide-ring hydrogels using polyrotaxanes have been developed as highly tough soft materials. However, they have never been used as biomaterials because of the lack of biocompatibility. Meanwhile, self-healing hydrogels are expected to improve fatigue resistance and extend the period of use. However, owing to the lack of high mechanical strength, they are limited in their use as biomaterials. Here we first developed a biocompatible self-healing/slide-ring hydrogel using glycol chitosan and a water-soluble polyrotaxane. We obtained excellent mechanical toughness and biocompatibility to promote the proliferation of human umbilical vein endothelial cells (HUVECs) encapsulated in the hydrogel. Owing to the rapid self-healing property, the cell-encapsulating gels adjusted arbitrarily, maintaining good cell proliferation function. Therefore, the slide-ring hydrogels enable the use of biomaterials for soft-tissue engineering.

Introduction

Hydrogels, a type of soft and wet material have been studied extensively for biomedical applications.[1] However, the practical applications of such hydrogels have been limited due to their mechanical weakness and brittleness. When developing biomimetic hydrogels for load-bearing soft tissue, this is a challenging issue to overcome this problem.[2] Recently, the slide-ring structure has been found to improve mechanical properties of polymer gels. A new approach to the polymer network structure has been developed using polyrotaxanes.[3] Okumura and Ito developed the first slide-ring material based on chemically cross-linked polyrotaxane.[2c] At the time of deformation, the cross-linking junctions of the figure-of-eight shapes were not immobilized at the polymer chains, but could move freely in the network to equalize the tension of the threading polymer chains in a manner similar to that of pulleys, involving the so-called “pulley effect”.[4] This particular property drastically changes the mechanical properties of polymeric materials, which is quite different from chemical hydrogels.[5] Slide-ring hydrogels are thought to be applicable to a variety of biomaterials such as tissue scaffolds.[6] This is because their excellent softness and biocompatibility are similar to those of mammalian skin, arteries, and so on.[7] This indicates that slide-ring hydrogels are suitable for use as substitutes of various kinds of biomaterials.[8] Despite their promising properties, slide-ring hydrogels have not been used as biomaterials. As the preparation method of slide-ring hydrogels usually involves fabrication under a harsh condition, the preparative environments are not biocompatible.[2c, 9] To the best of our knowledge, no reports have been published about slide-ring hydrogels in terms of their application as biomaterials, so there is a need for research in this area.[10]

The self-healing property of hydrogels is another important factor for improving fatigue resistance and maintaining stable functionality or extended periods of use. Dynamic covalent bonds combine both the reversibility of non-covalent cross-linking and the stability of covalent cross-linking in a single system, conferring the self-healing feature to the hydrogels.[11] Harada and colleagues reported on self-healing slide-ring materials based on polyrotaxane connected by dynamic covalent bonds between boronic acid and diol compounds.[12] However, in that study, there is no mention of the mechanical properties of slide-ring hydrogels. Moreover, the group prepared the hydrogel in an organic solvent, which also bears a risk of toxicity for biomedical applications.

In this study, we report the preparation of hydroxypropylated polyrotaxane aldehyde/glycol chitosan slide-ring hydrogels (HP-PRX-ALD/glycol chitosan (GC) gels) via the formation of a Schiff-base cross-linking network in mild conditions. The resulting hydrogels demonstrated soft and excellent mechanical properties because of the “pulley effect”. The HP-PRX-ALD/GC gels exhibited fast and efficient self-healing behavior under physiological conditions without any external stimuli. The complete degradation time was around 3 days, which could be controllable by crosslinking amount of HP-PRX-ALD. They could easily encapsulate human umbilical vein endothelial cells (HUVECs), and the HUVECs-encapsulating hydrogels were transformed into other shapes due to their self-healing properties, like a puzzle. The HUVECs were proliferated well for 5 days even though the hydrogels were degraded within 3 days, suggesting that the HP-PRX-ALD/GC gels are applicable for biomedical applications such as medical sealant devices[13] and neo-tissue growth support. [14]

Results

The hydroxypropylated polyrotaxane-bearing aldehydes (HP-PRX-ALD) were synthesized by a three-step procedure (Figure S2). First, we prepared a polyrotaxane, according to a previous report.[8] The ^{1}H NMR spectrum supported the success of the synthesis, and the average number of α-CD molecules per chain was determined to be ca. 95–115 (Figure S3). An aldehyde group was simply introduced by using Dess–Martin periodinane (DMP), which induces the mild oxidation of alcohols of α-CD. To obtain a water-soluble PRX, hydroxypropyl groups were randomly substituted for the hydroxyl groups of the α-CDs in the PRX. The ^{1}H NMR spectrum indicated that the average levels of oxidation and hydroxypropylation per α-CD molecule were ca. 1 and ca. 2, respectively (Figure S4, S5).

As shown in Figure 1, when HP-PRX-ALD was mixed with GC in distilled water, transparent HP-PRX-ALD/GC gels were formed. The formation of hydrogels was attributed to the Schiff-base reaction between the amine groups on GC and aldehyde groups along with the HP-PRX-ALD chains, which is in good agreement with the hydrogel formation by mixing oxidized dextran (ODEX) and GC (Figure S1). [15] As the HP-PRX-ALD/GC gels were prepared by simply mixing two aqueous solutions, the gelation

[a] Dr. I. S. Cho, Prof. Dr. T.Ooya
Department of Chemical Science and Engineering, Graduate School of Engineering, Kobe University, Kobe, Japan

Supporting information for this article is given via a link at the end of the document.

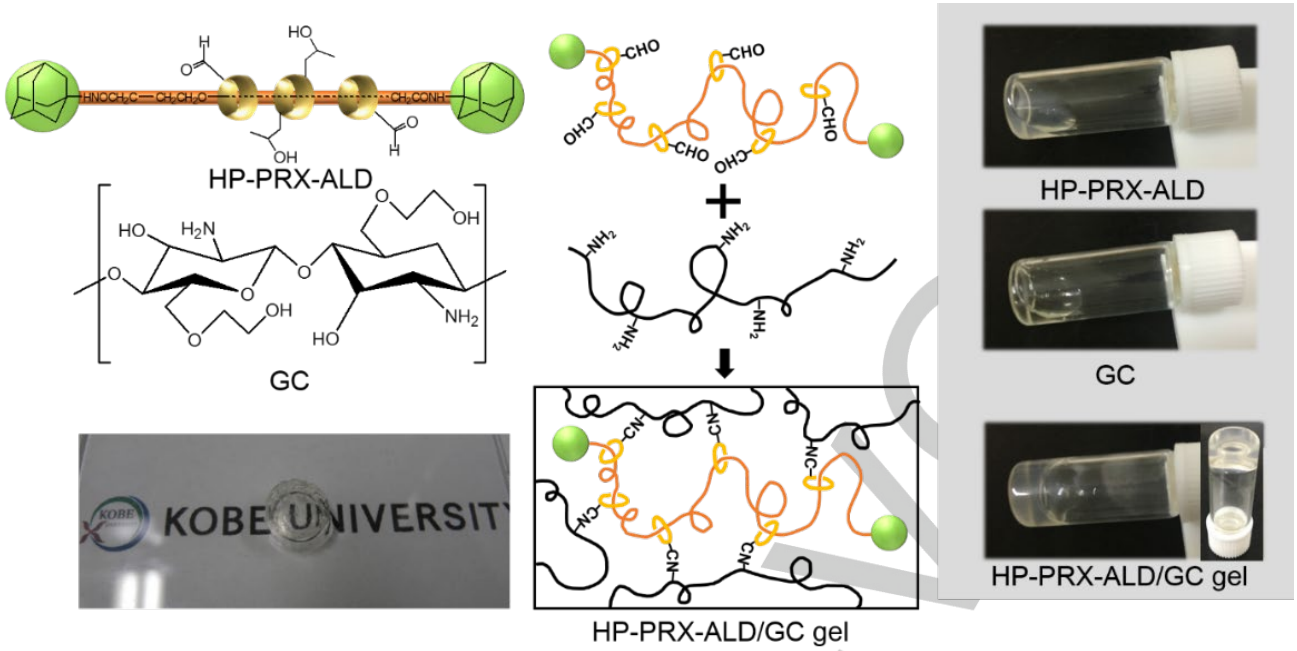

Figure 1. Construction of the slide-ring hydrogel prepared by just mixing hydroxypropylated polyrotaxane aldehydes (HP-PRX-ALD) and glycol chitosan (GC) in an aqueous solution.

speed and time of the mixed solution should be important factors of biomedical applications such as wound healing. The dependences of gelation speed and time of the HP-PRX-ALD/GC gels were determined by rheological analysis. The results of time-sweep rheological analysis indicate the transition of the HP-PRX-ALD/GC from a liquid phase to a solid phase with showing plots crossing of the storage (G`) and loss modulus (G``), which is defined as the gel point (Figure S6 A). The gelation speed and time were modulated by adjusting the concentration of HP-PRX-ALD. The gelation time decreased with increasing HP-PRX-ALD concentration. HP-PRX5-ALD/GC showed the longest gelation time (1383 s). With an increase of the HP-PRX-ALD concentration to 10 wt%, the gelation time decreased to 165 s (Table S1). This indicates that the high HP-PRX-ALD concentration increased the likelihood of encountering reactive groups on polymer chains and thus increased the probability of reaction among these groups. The Schiff-base formation was confirmed by FT-IR measurements (Figure S5B). We observed the characteristic absorption band attributed to the newly formed Schiff-base linkage (-C=N-) at 1605 cm^{-1}, suggesting that the coupling reaction occurred between -CHO of HP-PRX-ALD and -NH_2 of GC. In the similar manner, ODEX/GC gel (without polyrotaxane structure) was prepared as a control. [15] Here, the feed ratio of amino groups of GC and aldehyde groups of ODEX or HP-PRX_{10}-ALD ([NH_2]/[CHO]) was 1:1.4 and 1:1.3, respectively, which was comparable in terms of the Schiff-base formation.

To compare the morphological characteristics of the ODEX/GC and HP-PRX-ALD/GC gels, we observed the cross-sectional morphologies of the lyophilized hydrogel samples by scanning electron microscopy (SEM) (Figure S7). The SEM image of the HP-PRX-ALD/GC gel and ODEX/GC showed a well-developed structure with similar pore size. Especially, HP-PRX-ALD/GC gels show a fibril structure, which was not observed in the ODEX/GC hydrogel. According to a previous report, such a fibril structure has been shown in a polyrotaxane-based hydrogel.[16] The formation of this structure signified stress localization. Thus, the propagation of fibrils as observed in the polyrotaxane-based hydrogel suggests that movable polymer chains enabled the gels to modulate the mechanical properties.

Swelling properties are among the most important characteristics for the cell matrix because a high swelling index increases the permeability of cellular nutrients. The swelling behavior of the HP-PRX-ALD/GC gels was induced by immersing the hydrogels in Dulbecco's phosphate-buffered saline (DPBS; pH 7.4) at 37°C (Figure S8A). The equilibrium state of the swelling was reached at 6 h, and all the HP-PRX-ALD/GC gels with different HP-PRX-ALD concentrations reached swelling ratio between 2562% and 3394% at the equilibrium state. The obtained swelling ratio (2562%–3394%) is sufficient to penetrate cells for 3D cell encapsulation, because the swelling ratio of most hydrogels for cell encapsulation was reported to be in the range of 1300%–1500%.[17]

Biodegradability of the HP-PRX-ALD/GC gels is another important factor for their use as biomaterials. The degradation behavior was monitored by the weight change of hydrogels with incubation in DPBS (pH 7.4) at 37°C (Figure S8B). After the incubation for 1 week, the weight ratios were 60% for HP-PRX_{10}-ALD/GC. Moreover, HP-PRX5-ALD/GC was completely degraded. Owing to the concentration dependence of HP-PRX-ALD, this was mainly due to the hydrolytic susceptibility of the Schiff-base linkage.

The mechanical properties of the swollen HP-PRX-ALD/GC gels were determined in compression, cyclic compression, and tensile tests as well as an anti-slicing experiment. The stress–strain curves (Figure 2A) showed that all the HP-PRX-ALD/GC gels exhibited greater strength than the ODEX/GC gel. The HP-PRX-ALD/GC gels did not have a yield point or breaking point during the compression process, indicating their lack of fragility. The HP-PRX-ALD/GC gels could be adjusted in terms of their maximum compression stress to a value between 0.54 and 11 MPa by controlling the concentration of HP-PRX-ALD in the hydrogels. As shown in Figure 2B, the HP-PRX_{10}-ALD/GC gel

achieved a maximum compression stress of 11 MPa, which was 733 times higher than that of the ODEX/GC gel (0.015 MPa). As shown in Figure 2C, Young's modulus of the HP-PRX$_{10}$-ALD/GC gel (19.4 kPa) was found to be about one-fifth of that of the ODEX/GC gel (92.9 kPa). This indicates that the low Young's modulus of the slide-ring gel results from the pulley effect.[18]

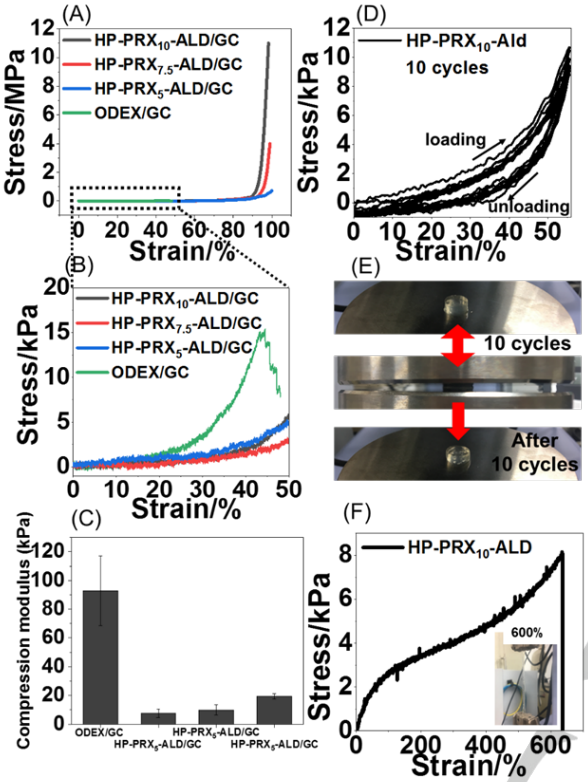

Figure 2. The excellent mechanical properties of swollen HP-PRX-ALD/GC gels. (A) and (B) Mechanical compression curves of the HP-PRX-ALD/GC gel at different concentrations and ODEX/GC hydrogel. (C) Young's modulus of the HP-PRX-ALD/GC gel and ODEX/GC hydrogel. (D) Cyclic compression test curves of the HP-PRX10-ALD/GC gel. (E) Digital images of the HP-PRX$_{10}$-ALD/GC gel during a cyclic compression test and after 10 cycles of compression. (F) Mechanical tensile curve of the HP-PRX10-ALD/GC gel.

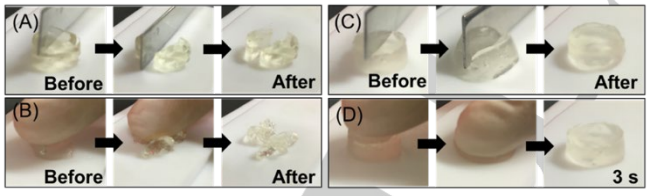

Figure 3. (A) An ODEX/GC hydrogel was easily cut in half with a spatula cutter or (B) readily broken by pressing. (C) Photographs show the strength of the HP-PRX$_{10}$-ALD/GC gel, which resisted slicing with a spatula cutter and recovered its shape. (D) Rapid recovery of the HP-PRX$_{10}$-ALD/GC gel after being pressed.

The hydrogels remained in their original shape without any damage on the surface after 10 loading–unloading cycles at a given strain of 55% (Figure 2D). Hysteresis loops were seen to indicate the process of relaxation of the polymer chains. The maximum stress of the hydrogels as well as the loops showed no obvious drop within the test of 10 cycles. Interestingly, the squeezed HP-PRX$_{10}$-ALD/GC gel recovered its original shape rapidly (Figure 2E). Moreover, a stress–strain curve of the HP-PRX$_{10}$-ALD/GC gel revealed that the maximum stretching length was reached at 630%, and the gel also displayed fair elasticity in this stretched state (Figure 2F). This result also indicates the typical characteristics of the pulley effect.[4]

The high stretch of the HP-PRX-ALD/GC gels due to the pulley effect was also qualitatively observed. As seen in Figure 3A and B, the ODEX/GC hydrogel was readily broken by either slicing with a cutter or pressing with a finger. However, the HP-PRX$_{10}$-ALD/GC gel resisted slicing with a spatula cutter even after reaching the maximum cutting depth (Figure 3C; see also Video S1). Moreover, the HP-PRX$_{10}$-ALD/GC gel pressed multiple times recovered its original shape within 3 s (Figure 3D; see also Video S2).

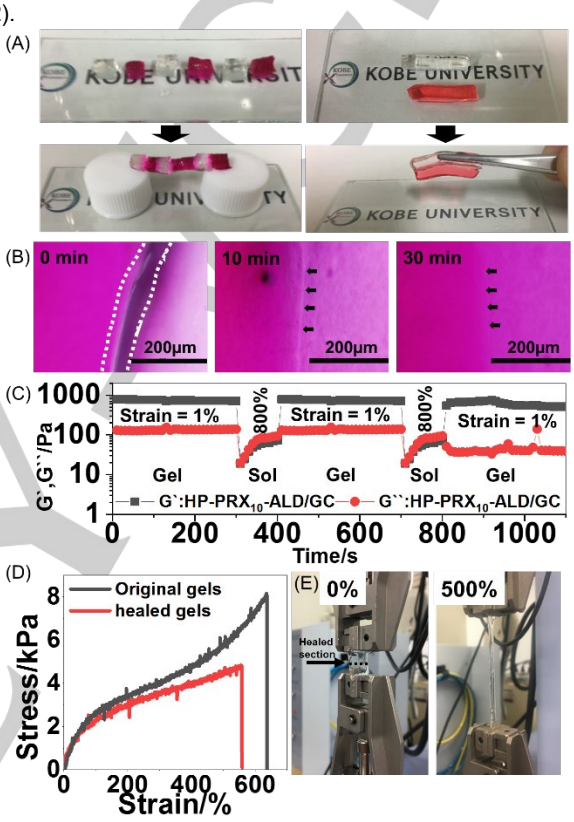

Figure 4. (A) Freshly cut HP-PRX$_{10}$-ALD/GC gel with the small columns and the self-healed cylinder bridging between two caps to support its own weight (Left). And prepared HP-PRX$_{10}$-ALD/GC gels are spliced and placed in a room temperature (Right). (B) Optical microscopy images of the HP-PRX$_{10}$-ALD/GC gel after being self-healed for 0, 10, and 30 min. (C) Self-healing ability of the HP-PRX$_{10}$-ALD/GC gel characterized by the continuous step strain measurements: A continuous step change of oscillatory strain between 800% and 1% under the same frequency (1 Hz) was applied to evaluate the strain-induced damage and healing of the hydrogel. (D) Tensile stress–strain curves of the original HP-PRX$_{10}$-ALD/GC gel and the healed HP-PRX$_{10}$-ALD/GC gel. (E) Elongated state of the healed HP-PRX$_{10}$-ALD/GC gel at 500% strain.

As the hydrogel network was constructed through the Schiff-base formation between HP-PRX-ALD and GC, the polymeric chains in the hydrogel network would be expected to de-cross-link and re-cross-link, resulting in their self-healing ability. To test this, freshly cut surfaces of the HP-PRX$_{10}$-ALD/GC gel were adhered to each other, and uncutted hydrogels were spliced each other. We constructed a bridge by connecting six blocks (Figure 4A). The HP-PRX$_{10}$-ALD/GC gel was sliced with a razor and three small columns were stained with rhodamine B to distinguish them easily. Then, the blocks were pushed together and stored at room temperature for 30 min. The cut samples were found to be well healed, where the self-healed cylinder was strong enough to hold

when suspended horizontally between two posts without any visible damage. Optical images clearly revealed the time course of the self-healing process (Figure 4B). The crack made by a blade healed gradually after 10 min and disappeared completely after 30 min. Rheology tests were performed to measure the elastic response of the self-healing hydrogels. Damage of the self-healing hydrogel after applying a high shear strain and healing at a low strain is shown in Figure 4C. Structure destruction was induced via the application of 800% strain for 100 s, which resulted in a decrease in the G‘ value of the self-healing HP-PRX_{10}-ALD/GC gel from approximately 785 to 19 Pa. The strain was then decreased to 1% for 200 s to allow the gel to recover. During the time under this low strain, the G′ value of the self-healing HP-PRX_{10}-ALD/GC gel recovered quickly to the initial value, and the hydrogel underwent a rapid sol-to-gel transition. The stress–strain curve of the healed HP-PRX_{10}-ALD/GC gel was further obtained by tensile testing (Figure 4D). The HP-PRX_{10}-ALD/GC gel was cut into two pieces, the two parts were placed in contact with each other for 30 min, and then, the healed gel was stretched to test the tensile strength. The stress–strain curves show that the self-healed HP-PRX_{10}-ALD/GC gel and the original samples shared mechanical properties. These results indicate that the HP-PRX_{10}-ALD/GC gel with excellent self-healing performance can effectively repair possible damage due to the reversibility of the Schiff-base linkage. The healed gel was well starched at 500% strain (Figure 4E).

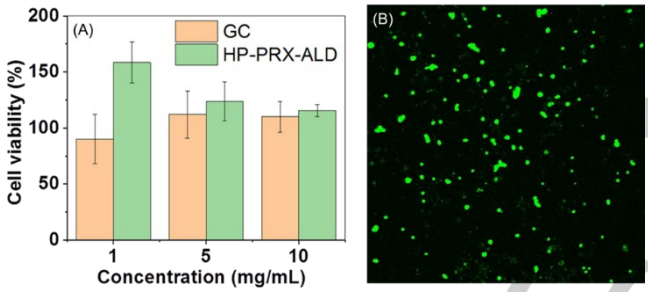

Figure 5. (A) In vitro cytotoxicity study of GC and HP-PRX-ALD/GC to observe cell viability as a function of concentration in fibroblast cells. (B) Live/dead imaging of encapsulated HUVECs within the HP-PRX_{10}-ALD/GC gel at 2 days.

To apply the HP-PRX-ALD/GC gels as biomaterials, they and their constituent polymers (i.e., HP-PRX-ALD and GC) should not be cytotoxic or exert harmful effects on any cellular function in their future applications.[19] To evaluate the present hydrogels as a potential cell matrix, the cytotoxicity of GC and HP-PRX-ALD was investigated by the MTT assay. The influence of GC and HP-PRX-ALD on the proliferation of NIH 3T3 fibroblasts was examined and is shown in Figure 5A. The results demonstrate that after 24 h, GC and HP-PRX-ALD at various concentrations showed low cytotoxicity on NIH 3T3 fibroblasts. Moreover, the cytocompatibility of the HP-PRX_{10}-ALD/GC gel was confirmed via a live/dead assay of HUVECs loaded inside the hydrogels (Figure 5B). The cells stained green are live cells, whereas those stained red are dead. The HUVECs were homogeneously dispersed in the HP-PRX_{10}-ALD/GC gel and the results indicated that most cells were alive. These results demonstrate that the HP-PRX-ALD/GC gel exhibits no cytotoxic.

Cell encapsulation has a number of advantages over 2D conventional cell culture, which include improved cell–cell contact and cell matrix interactions. These encapsulation techniques depend on the properties of the hydrogels defining the mechanical and chemical environment surrounding the cells. In this case, cells are encapsulated in prepared slide-ring gels since they show mechanical properties similar to those of biomaterials, such as mammalian skin, vessels, and tissues. In particular, we investigated how the mechanical properties of HP-PRX-ALD/GC gels affected cell spreading and morphology 5 days after encapsulation. We used HUVECs as a cellular model to illustrate the relationship between the softness of the hydrogel and the spreading of the encapsulated cells.

As the HP-PRX_{10}-ALD/GC gel is capable of self-healing without any treatment, a variety of sophisticated hydrogel structures could be constructed that are not possible in direct gelation processes. Figure 6A shows a simple cross shape of HUVECs encapsulated in the HP-PRX_{10}-ALD/GC gel made by cutting each end face using a sterile blade and directly connecting it in the opposite position to allow healing. The HP-PRX_{10}-ALD/GC gel was healed in an incubator at 37 °C and 5% CO_2 for 1 h to form now hydrogel constructs. At certain time points (days 1, 3, and 5), a confocal tile scan was performed, centered on the interface of the healed section. HUVECs were able to cross, spread, and connect at the healed section.

To confirm the HUVEC morphology in the HP-PRX_{10}-ALD/GC gel, we performed CD31 staining using Alexa Fluor® 594 anti-human CD31 antibody. As shown in Figure 6B, HUVECs encapsulated in the ODEX/GC gel had no spreading 3D structure of the gel. On the other hand, the HP-PRX_{10}-ALD/GC gel showed a significant increase in HUVEC spreading in 3D constructs. This was due to the fact that cells tend not to spread, elongate, and migrate when they are encapsulated in structures exhibiting high stiffness (over 25 kPa).[20] In addition, the fluorescent intensity of CD31 was in agreement with the finding that the proliferation increased significantly with increasing culture time (1, 3, and 5 days) (Figure 6C). When cultivated for 5 days, the proliferation rate of the cells encapsulated in the HP-PRX_{10}-ALD/GC gel was significantly higher than that of the ODEX/GC gel. These results indicate that the HP-PRX_{10}-ALD/GC gel promoted the proliferation of HUVECs in a 3D environment.

Discussion

Several attempts have been made to prepare excellent soft, and stretchable hydrogels using polyrotaxane (PRX) as a cross-linkable polymer. We first prepared a slide-ring hydrogel using GC and PRX modified by oxidation and hydroxylpropylation, which contains aldehyde and hydroxypropyl groups.

The unmodified PRX, prior to oxidation and hydroxylpropylation, forms aggregates in pure water due to hydrogen bonding between the hydroxyl groups on α-CDs. In this state, α-CDs cannot move along the PEG chains and the pulley effect is limited. As a result, the PRX slide-ring gel became opaque and did not exhibit unique slide-ring properties (softness, strech). Therefore, the PRX should be fully dissolved during the cross-linking step to obtain homogeneous networks. In fact, PRX is soluble only in a few solvents, such as DMSO, high-pH aqueous solutions, some ionic liquids, and mixtures of organic amides and lithium salts. Thus, to date, no reports of biomedical applications of the slide-ring hydrogels have been published. The synthesized HP-PRX-ALD shows excellent water solubility even at a high concentration (10 wt%). This indicates that our synthesized HP-PRX-ALD can easily and homogeneously fabricate a slide-ring gel by mixing with GC solution under physiological conditions.

The movable cross-linking junctions in HP-PRX-ALD/GC gels conferred unique mechanical behavior due to the pulley effect (Figures 2 and 3). These results demonstrate that the HP-PRX-ALD/GC gels are fatigue-resistant, elastic, anticompressing, and can recover their shape.

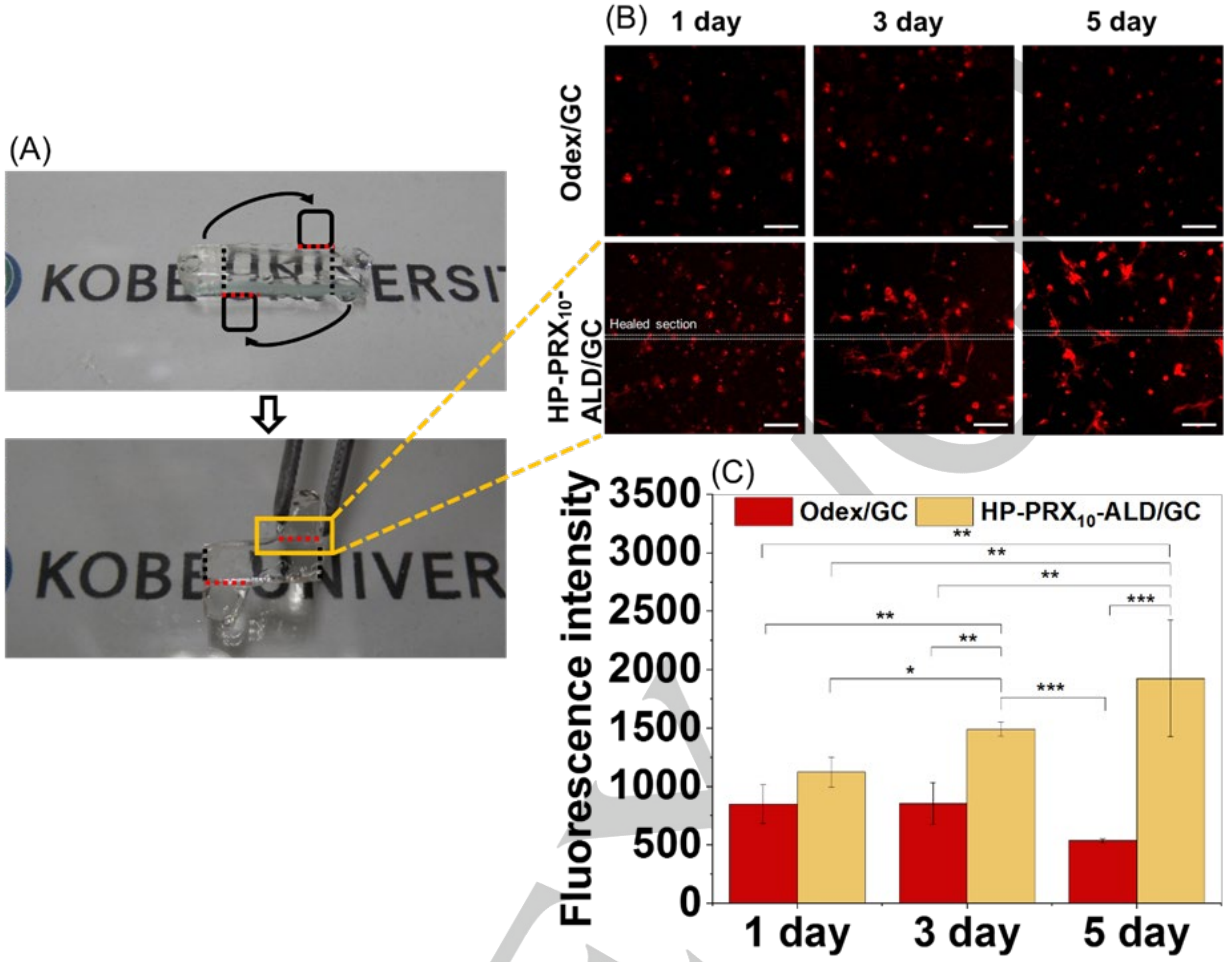

Figure. 6. (A) Photographs of the HP-PRX_{10}-ALD/GC gel made into a cross shape via self-healing properties. (B) Confocal microscopy images with the healed section view on immunostaining for CD31 (red). Scale bar 100 μm. (C) The fluorescence intensity of Alexa Fluor® 594 anti-human CD31-labeled HUVECs within the ODEX/GC and HP-PRX_{10}-AD/GC gels were determined using NIH ImageJ software to assess the proliferation of HUVECs at different culture times.

The free junction model shows that HP-PRX-ALD/GC gels exhibit a significantly small amount of stress at a low compression ratio, and the stress increases drastically at a compression rate over 85%. In contrast, in the fixed junction model, ODEX/GC gels showed that the normal stress increased gradually with compression, with breaking occurring rapidly (Figure 2). Here, the apparent crosslinking density between HP-PRX_{10}-ALD/GC gel and ODEX/GC gel was almost the same becasue, when both the gels were prepared, the the feed ratio of amino groups of GC and aldehyde groups of ODEX or HP-PRX_{10}-ALD was the same (1:1.3-1.4) with the same number of aldehyde in ODEX (ca. 92-128) and HP-PRX_{10}-ALD (ca. 95-115) This indicates that ODEX/GC gel is fragile in nature, so Young's modulus of HP-PRX-ALD/GC gels is lower than that of ODEX/GC gels (Figure 2C). It has been reported that cells tend not to spread when they are encapsulated in structures exhibiting an elastic modulus over 25 kPa[20]. The results of Young's modulus of the HP-PRX_{10}-ALD/GC gel (19.4 kPa) (Figure. 2C) suggest that this gel is suitable for use as a 3D cell culture. In fact, Young's modulus of the HP-PRX-ALD/GC gels (7.5–19.4 kPa) is in good agreement with that required for stem cell differentiation on a 3D hydrogel matrix[21].

The most beneficial feature of the HP-PRX-ALD/GC gels is the associated HUVEC proliferation after self-healing (Figure 6). Compared with the case of the ODEX/GC gel, the HP-PRX_{10}-ALD/GC gel after self-healing did not disturb the proliferation of HUVECs (Figure 6B), suggesting the appropriate stiffness of the hydrogel[20-21]. Thus, the HP-PRX_{10}-ALD/GC gel could safely encapsulate HUVECs, and the cell-encapsulating gels can adjust arbitrarily by the self-healing properties.

Conclusion

We report a biocompatible slide-ring hydrogel based on HP-PRX-ALD and GC via convenient Schiff-base linkage formation without the use of any organic solvents. Unlike chemically cross-linked hydrogels, this hydrogel shows extreme softness, stretchability because of the pulley effect. Schiff-base linkage, one of the dynamic covalent bonds, imparts the capacity for self-healing on the hydrogel, as confirmed by the macroscopic self-healing test, rheological recovery test, and tensile test. Moreover, the hydrogel promoted good cell proliferation and easy adjustment of the spatial portion of the cells via self-healing

properties. We anticipate that this HP-PRX-ALD/GC slide-ring hydrogel might offer diverse applications in biomedical fields.

Experimental Section

Materials

Polyethylene glycol 35000 (PEG35000), 2,2,6,6-tetramethylpiperidin-1-yl)oxyl (TEMPO), sodium hydroxide solution 50% in H_2O, and 1-adamantylamine were purchased from Sigma-Aldrich (Tokyo, Japan). GC, DP≥ 200), ethanol, dichloromethane, BOP reagent, and Dess‐Martin periodinane (DMP) were purchased from Fujifilm Wako Pure Chemical Industries, Ltd. (Osaka, Japan). Sodium bromide (NaBr), sodium hypochlorite (NaClO), ethyldiisopropylamine (EDIPA), Dextran (DEX, M_n=50,000-70,000), sodium periodate, methanol, and dimethylformamide (DMF) were purchased from Nacalai Tesque Co. Ltd. (Kyoto, Japan). Propylene oxide, *tert*-butyl carbazate and dimethyl sulfoxide were purchased from Tokyo Chemical Industry Co., Inc. (Tokyo, Japan). α-Cyclodextrin (α-CD) was purchased from Junsei Chemical Co., Ltd. (Tokyo, Japan). Alexa Fluor® 594 anti-human CD31 antibody was purchased from BioLegend (San Diego, CA, USA). Endothelial cell basal medium 2 was purchased from Promo Cell (city, Germany). Endothelial cell growth medium 2 kit was purchased from TaKaRa Bio Inc. (Shiga, Japan).

Synthesis of polyrotaxane (PRX) with PEG-carboxylic acid

Oxidation of terminal hydroxyl groups in PEG35000 was carried out by TEMPO. PEG35000 (10.0 g) was dissolved in 100 mL of distilled water with TEMPO (100 mg) and sodium bromide (100 mg). To this solution, 10 mL of an aqueous solution of sodium hypochlorite was added, and the resulting mixture was stirred at room temperature for 30 min. A total of 10 mL of ethanol was added to decompose an excess of the sodium hypochlorite to terminate the reaction, followed by acidification with HCl to pH < 2 and three extractions with 100-mL aliquots of methylene chloride. The combined methylene chloride layers were dried under reduced pressure and dissolved in 250 mL of hot ethanol, followed by precipitation in a freezer overnight. Recrystallization with ethanol twice and vacuum-drying gave pure PEG-COOH.

A total of 3.0 g of prepared PEG-COOH was dissolved in 100 mL of distilled water, and further with 12.0 g of α-CD. The resulting mixture was stirred for 2 h at room temperature and the mixture was kept in a refrigerator overnight, giving a white paste-like inclusion complex. The prepared dispersion of pseudopolyrotaxane was dried by a freeze-dryer. Adamantanamine (0.16 g) was dissolved in dehydrated DMF (80 mL) at room temperature. Then, the freeze-dried complex (14.0 g) obtained was added to the solution, and the solution was promptly shaken well. Subsequently, a solution of 0.48 g of BOP reagent in 10 mL of dehydrated DMF was added to the solution. Furthermore, 0.19 mL of EDIPA in 10 mL of dehydrated DMF was added to the solution, and the slurry-like mixture obtained was stirred for 3 h and allowed to react at 4 °C overnight. The mixture was then centrifuged twice with DMF/methanol (1:1) and twice with methanol. The resulting solid was dissolved in DMSO (80 mL) and precipitated in water (800 mL). The precipitate was washed repeatedly with distilled water by centrifugation and lyophilized to give polyrotaxane as a white solid. The number of α-CD molecules per chain calculated according to the ^{1}H-NMR peak was 100–115.

Synthesis of polyrotaxane aldehyde (PRX-ALD)

To prepare polyrotaxane aldehydes (PRX-ALD), 1.0 g of polyrotaxane and 0.696 g of DMP were dissolved in 50 mL of DMSO. Then, the mixture was subjected to magnetic stirring for 24 h at room temperature and the reaction mixture was dropped into 200 mL of acetone, stirred for 1 h, and then left to stand for 2 h in a freezer. The solution was dialyzed in distilled water for 3 days and the precipitate was collected and freeze-dried to give PRX-ALD as a white solid. The degree of oxidation was determined by quantifying the aldehyde groups formed by *tert*-butyl carbazate via carbazone formation. The average number of oxidation per α-CD molecule was determined to be ca. 1.0.

Synthesis of hydroxylpropylated polyrotaxane aldehydes (HP-PRX-ALD)

The PRX-ALD (1.0 g) obtained was allowed to react with propylene oxide (12.48 mL) in 1 N NaOH solution (100 mL) at room temperature for 24 h. The reaction solution was neutralized by adding HCl solution and dialyzed against distilled water for 3 days, and then lyophilized to collect HP-PRX-ALD in white sponge form.

Synthesis of oxidized dextran (ODEX) [15]

Oxidized dextran (ODEX) was prepared by first dissolving 2 g of DEX in 160 mL of distilled water and then the dropwise addition of 1.03g of NaIO4 dissolved in 40 mL of distilled water. This mixture was stirred at room temperature for 24 hr, followed by an equimolar amount of diethylene glycol was added to quench the unreacted NaIO4 and stirred for 1 hr. The ODEX mixture was then dialyzed against distilled water for 1 day using a dialysis membrane (MWCO 6,000-8,000), and the pure ODEX was obtained in a powder form after lyophilization (yield 65%). The oxidation degree of ODEX was determined by quantifying the aldehyde groups formed by *tert*-butyl carbazate via carbazone formation. The degree of oxidation of DEX was measured to be 33 %, which means that the number of oxidation units per DEX molecule was ca. 92-128 .

Preparation of the ODEX/GC gel[15]

Aqueous ODEX and GC solutions of 2 wt % in distilled water were each prepared and stored at 4 °C before use. To prepare hydrogels Odex solutions were mixed with GC solutions in a weight ratio of 1:1. The mixtures were gently vortexed for 10s, and the mixture was maintained at 37 °C for gelation. The gelation time of the ODEX/GC hydrogels were 121 s.

Preparation of the HP-PRX-ALD/GC gel

Aqueous HP-PRX-ALD solutions of 5, 7.5, and 10 wt% in distilled water were prepared. To prepare hydrogels, 5, 7.5, and 10 wt% HP-PRX-ALD solutions were mixed with 5 wt% GC solution at a ratio of 1:1. The mixtures were stirred gently for 10 s and then maintained at 37 °C for gelation; they were named HP-PRXX-ALD/GC gels, where “X” represents the concentration of HP-PRX-ALD. The gelation time of the hydrogels was observed using a rheometer (MCR-302; Anton Paar, Graz, Austria). To investigate the gelation kinetics of aqueous HP-PRX-ALD/GC,

time-sweep tests were performed at a constant oscillatory frequency (10 rad/s) by using a rheometer in plate-plate geometry (20 mm in diameter, with a gap of 1 mm) at 37 °C. The samples were placed on the test plate immediately after mixing and the measurement was started after 1 min. For GC/HP-PRX_{10}-ALD the theoretical [NH_2]/[CHO] ratio was approximately 1:1.3.

Morphology of the HP-PRX-ALD/GC gel

To observe the morphological structure of the HP-PRX-ALD/GC gel, cylindrical hydrogels (10 mm diameter × 5 mm thickness) were lyophilized under a vacuum at −50 °C. Dried hydrogels were obtained and fractured along the middle to expose their cross-sections. Then, Pt-coated cross-sections of the hydrogels were observed by SEM.

Swelling behavior of the hydrogel

For swelling rate analysis, HP-PRXx-ALD/GC hydrogels with different HP-PRX-ALD concentrations (5, 7.5, and 10 wt%) were created as disks. These hydrogels were freeze-dried, followed by immersion in PBS (0.01 M) at 37°C. After excess surface water was removed with filter paper, the swollen samples were weighed at specified time intervals. All experiments were performed in triplicate. The swelling ratio of a hydrogel was calculated using the following equation (1):

$$\text{Swelling ratio (\%)} = (M_w\text{-}M_d)/M_d \times 100 \qquad (1)$$

where M_w is the swollen hydrogel weight and M_d is the dried hydrogel weight.

***In vitro* degradation**

To evaluate the degradability of the hydrogels, in vitro degradation tests were carried out. The degradation process was monitored by measuring the weight of a hydrogel placed in a conical tube containing 30 mL of PBS (0.01 M). At specified time intervals, hydrogels were removed from the tubes, wiped carefully using filter paper, and weighed. The in vitro degradation of the hydrogels was calculated using Equation (2):

$$\text{Mass loss (\%)} = M_t/M_i \times 100 \qquad (2)$$

where M_i is the initial weight of the hydrogel and M_t is the weight of the hydrogel that has been degraded.

Mechanical testing

Compressive and tensile stress–strain measurements were performed using an automatic recording universal testing instrument (Autograph AGS-X; Shimadzu Co., Kyoto, Japan). A cylindrical sample with a diameter of 10 mm and height of 5 mm was set on the lower plate and compressed by the upper plate, which was connected to a load cell, at a strain rate of 1 min^{-1}. For the cyclic compression test, the cyclic hydrogels were compressed at a constant speed of 1 mm min^{-1}, with compression strain between 0% and 55% for 10 cycles. Tensile tests were performed using a square-shaped specimen with width, height, and thickness of 10, 10, and 1 mm, respectively. The sample was held on the instrument between clamps, and the tensile stress was loaded at a strain rate of 1 min^{-1}.

Self-healing evaluation

To test the self-healing ability of the HP-PRX-ALD gels, we performed microscopic and macroscopic observations. The whole hydrogel was cut into multiple pieces, which were then physically placed together at room temperature for 30 min. Rheological analysis of the hydrogel was carried out to monitor the self-healing process qualitatively. Continuous step strain measurements were carried out to test the rheological recovery behavior of the hydrogel. The strain was changed from 1% to 800% at a constant frequency (1.0 Hz) and the process was repeated twice.

Cytotoxicity evaluation

To evaluate the viability of cells cultured with GC and HP-PRX-ALD, the 3-(4,5-dimethylthiazol-2-yl)-2,5-diphenyltetrazolium bromide (MTT) assay was performed. For this, NIH 3T3 fibroblasts were seeded in a 96-well plate (5 × 103 cells/well) and incubated at 37°C and 5% CO_2 for 24 h. The cells were incubated with various concentrations of GC and HP-PRX-ALD (1.0, 5.0, and 10.0 mg/mL), followed by incubation for 1 day at 37 °C. MTT solution (10 µL) was added to each well. After incubation for 2 h at 37 °C, the optical intensity was measured using a microplate reader (SH-9000; CORONA ELECTRIC, city, Japan). The cell viability was visually measured using the Live/Dead assay kit (Abcam, city, MA, USA). HUVECs were encapsulated in HP-PRX_{10}-ALD/GC gels by suspending the cells in the HP-PRX-ALD solution and then mixing with GC solution. The precursor solution was then pipetted into a four-chamber plate (1 × 10^6/100 µL) and incubated until cross-linking. The cells encapsulated within the HP-PRX_{10}-ALD/GC gel were cultured in endothelial cell basal medium at 37 °C with a 5% CO_2 atmosphere for 1 day. Subsequently, live and dead cells were stained with the live/dead assay kit and visualized with a confocal microscope imaging system.

Quantification of cell proliferation

HUVECs were suspended in HP-PRX_{10}-ALD solution at a concentration of 1.0 × 10^6/100 µL, after which they were mixed with GC solution and pipetted into a rod-like mold. Each side of the rod-like hydrogels was cut and attached to new interfaces, after which newly modulated hydrogel was incubated at 37 °C until self-healing. As a control, ODEX/GC gel was prepared, which is a traditional chemically cross-linked hydrogel. The modulated hydrogel was then placed inside a four-chamber plate and cultured in endothelial cell basal medium at 37 °C with a 5% CO_2 atmosphere for 5 days, during which the culture medium was changed every other day. After cells had been cultured for 1, 3, and 5 days in the HP-PRX_{10}-ALD/GC gel, immunostaining of the CD31 membrane protein was performed on the HUVEC-encapsulating hydrogel. For CD31, samples were fixed in 4% w/v paraformaldehyde for 30 min and exposed to 0.1% (v/v) Triton X-100 in DPBS for 30 min to permeabilize the cell membrane. On permeabilization, the samples were blocked in 10 wt% bovine serum in DPBS for 1 h at 37 °C and incubated with human anti-CD31 antibodies at 1/100 dilution. Fluorescent images of the cells were captured in self-healed regions. The fluorescence intensity of cells was determined using NIH ImageJ software to assess the proliferation of HUVECs at different culture times (days 1, 3, and 5).

Acknowledgements

We are grateful to Kazune Oda (Kobe University, Japan) for mechanical testing. We thank Prof. Dr. Michiya Matsuzaki (Osaka University, Japan) for kindly providing the HUVECs. We also gratefully acknowledge financial support in the form of Grant-in-Aid for JSPS Research Fellows (JSPS KAKENHI grant number 17J09992) and funding from Izumi Science and Technology Foundation, Japan (2018-J-75).

Keywords: Polyrotaxane • Gels • Cyclodextins • Self-healing • Cell adhesion

[1] a) W. Ha, J. Yu, X.-y. Song, J. Chen and Y.-p. Shi, *ACS applied materials & interfaces* **2014**, *6*, 10623-10630; b) Y. Jiang, J. Chen, C. Deng, E. J. Suuronen and Z. Zhong, *Biomaterials* **2014**, *35*, 4969-4985; c) B. Jeong, Y. H. Bae and S. W. Kim, *Journal of controlled release* **2000**, *63*, 155-163.

[2] a) J. P. Gong and Y. Osada in *Soft and wet materials: from hydrogels to biotissues*, Springer, **2010**, pp. 203-246; b) Y. Zhao, T. Nakajima, J. J. Yang, T. Kurokawa, J. Liu, J. Lu, S. Mizumoto, K. Sugahara, N. Kitamura and K. Yasuda, *Advanced Materials* **2014**, *26*, 436-442; c) Y. Okumura and K. Ito, *Advanced Materials* **2001**, *13*, 485-487; d) T. Sakai, T. Matsunaga, Y. Yamamoto, C. Ito, R. Yoshida, S. Suzuki, N. Sasaki, M. Shibayama and U.-i. Chung, *Macromolecules* **2008**, *41*, 5379-5384.

[3] P.-G. de Gennes, *Physica A: Statistical Mechanics and its Applications* **1999**, *271*, 231-237.

[4] C. Liu, H. Kadono, K. Mayumi, K. Kato, H. Yokoyama and K. Ito, *ACS Macro Letters* **2017**, *6*, 1409-1413.

[5] K. Ito, *Polymer Journal* **2011**, *44*, 38.

[6] T. Ichi, J. Watanabe, T. Ooya and N. Yui, *Biomacromolecules* **2001**, *2*, 204-210.

[7] K. Ito, *Current Opinion in Solid State and Materials Science* **2010**, *14*, 28-34.

[8] J. Araki, C. Zhao and K. Ito, *Macromolecules* **2005**, *38*, 7524-7527.

[9] J. Araki and K. Ito, *Soft Matter* **2007**, *3*, 1456-1473.

[10] Y. Liang, J. Xue, B. Du and J. Nie, *ACS applied materials & interfaces* **2019**, *11*, 5441-5454.

[11] a) S. J. Rowan, S. J. Cantrill, G. R. Cousins, J. K. Sanders and J. F. Stoddart, *Angewandte Chemie International Edition* **2002**, *41*, 898-952; b) J.-M. Lehn, *Chemical Society Reviews* **2007**, *36*, 151-160; c) G. Deng, C. Tang, F. Li, H. Jiang and Y. Chen, *Macromolecules* **2010**, *43*, 1191-1194.

[12] M. Nakahata, S. Mori, Y. Takashima, H. Yamaguchi and A. Harada, *Chem* **2016**, *1*, 766-775.

[13] Y. Z. Bu, L. C. Zhang, G. F. Sun, F. F. Sun, J. H. Liu, F. Yang, P. F. Tang and D. C. Wu, *Advanced Materials* **2019**, *31*, 1901580.

[14] S. L. Sridhar, M. C. Schneider, S. Chu, G. de Roucy, S. J. Bryant and F. J. Vernerey, *Soft Matter* **2017**, *13*, 4841-4855.

[15] I. S. Cho and T. Ooya, *Journal of Biomaterials Science-Polymer Edition* **2018**, *29*, 145-159.

[16] K. Kato, K. Nemoto, K. Mayumi, H. Yokoyama and K. Ito, *ACS applied materials & interfaces* **2017**, *9*, 32436-32440.

[17] a) T. Zhao, D. L. Sellers, Y. Cheng, P. J. Horner and S. H. Pun, *Biomacromolecules* **2017**, *18*, 2723-2731; b) H. Park, X. Guo, J. S. Temenoff, Y. Tabata, A. I. Caplan, F. K. Kasper and A. G. Mikos, *Biomacromolecules* **2009**, *10*, 541-546.

[18] H. Gotoh, C. Liu, A. B. Imran, M. Hara, T. Seki, K. Mayumi, K. Ito and Y. Takeoka, *Science advances* **2018**, *4*, eaat7629.

[19] Z. Wei, J. Zhao, Y. M. Chen, P. Zhang and Q. Zhang, *Scientific reports* **2016**, *6*, 37841.

[20] C. Colosi, S. R. Shin, V. Manoharan, S. Massa, M. Costantini, A. Barbetta, M. R. Dokmeci, M. Dentini and A. Khademhosseini, *Advanced materials* **2016**, *28*, 677-684.

[21] K. Wingate, W. Bonani, Y. Tan, S. J. Bryant and W. Tan, *Acta biomaterialia* **2012**, *8*, 1440-1449.

Entry for the Table of Contents

RESEARCH ARTICLE

The slide-ring hydrogels with self-healing ability were developed as biomaterials. Human umbilical vein endothelial cells encapsulated in the hydrogel showed increased proliferation. The gel's ability to self-heal promoted this cell proliferation. This content highlights the value of using slide-ring hydrogels for biomaterials for soft-tissue engineering.

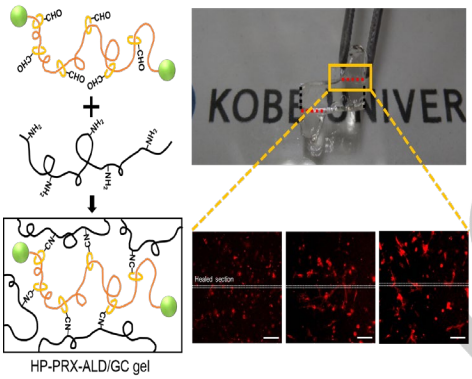

*Ik Sung Cho, Tooru Ooya**

Page No. – Page No.

Cell-Encapsulating Hydrogel Puzzle: Polyrotaxane-Based Self-Healing Hydrogels

SUPPORTING INFORMATION

Abstract: Slide-ring hydrogels using polyrotaxanes have been developed as highly tough soft materials. However, they have never been used as biomaterials because of the lack of biocompatibility. Meanwhile, self-healing hydrogels are expected to improve fatigue resistance and extend the period of use. However, owing to the lack of high mechanical strength, they are limited in their use as biomaterials. Here we first developed a biocompatible self-healing/slide-ring hydrogel using glycol chitosan and a water-soluble polyrotaxane. We obtained excellent mechanical toughness and biocompatibility to promote the proliferation of human umbilical vein endothelial cells (HUVECs) encapsulated in the hydrogel. Owing to the rapid self-healing property, the cell-encapsulating gels adjusted arbitrarily, maintaining good cell proliferation function. Therefore, the slide-ring hydrogels enable the use of biomaterials for soft-tissue engineering.

DOI: 10.1002/anie.2019XXXXX

SUPPORTING INFORMATION

Table of Contents

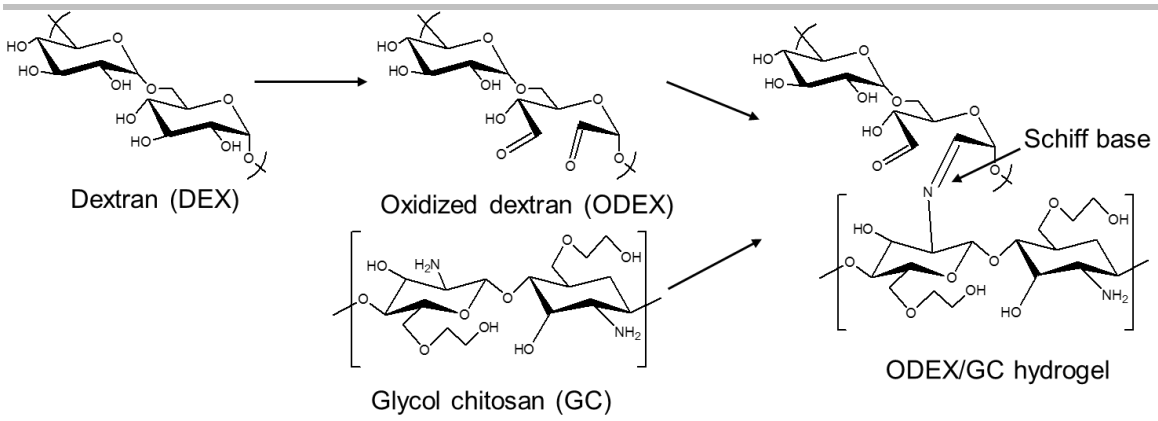

Figure S1. Synthetic scheme of periodate oxidation of dextran and preparation of ODEX/GC hydrogel via the Schiff-base linkage with glycol chitosan.

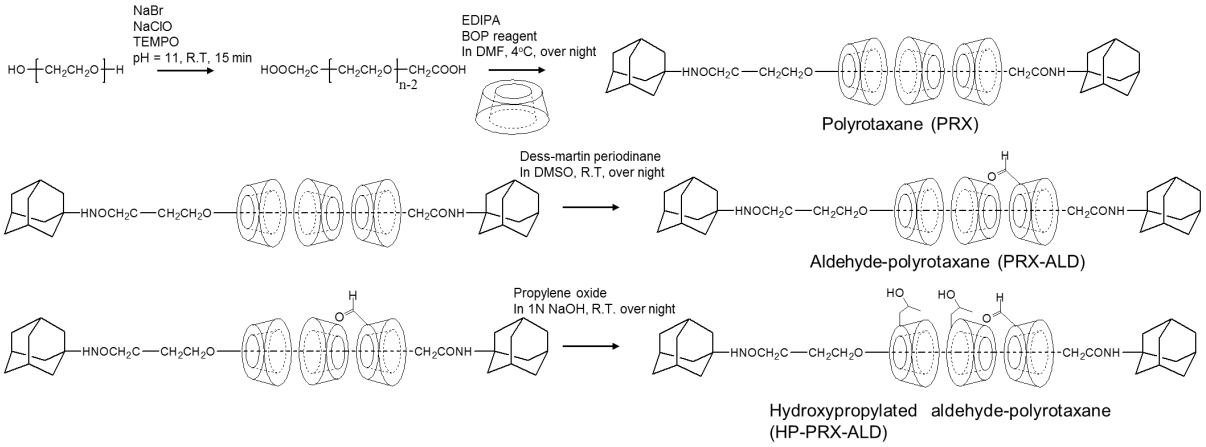

Figure S2. Synthesis of HP-PRX-ALD from PRX through the oxidation and hydroxypropylation.

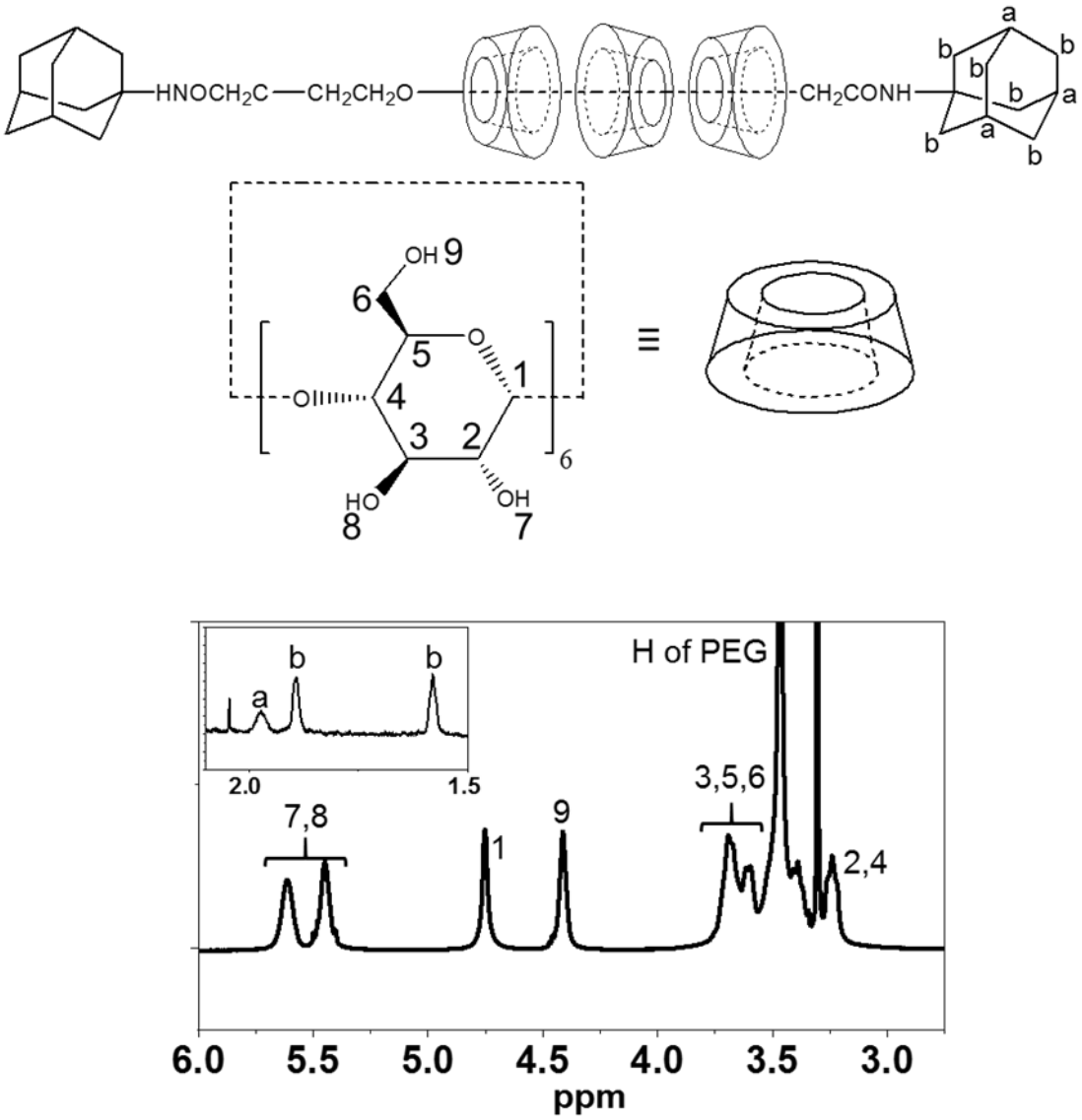

Figure S3. ^{1}H-NMR spectra of the polyrotaxane.

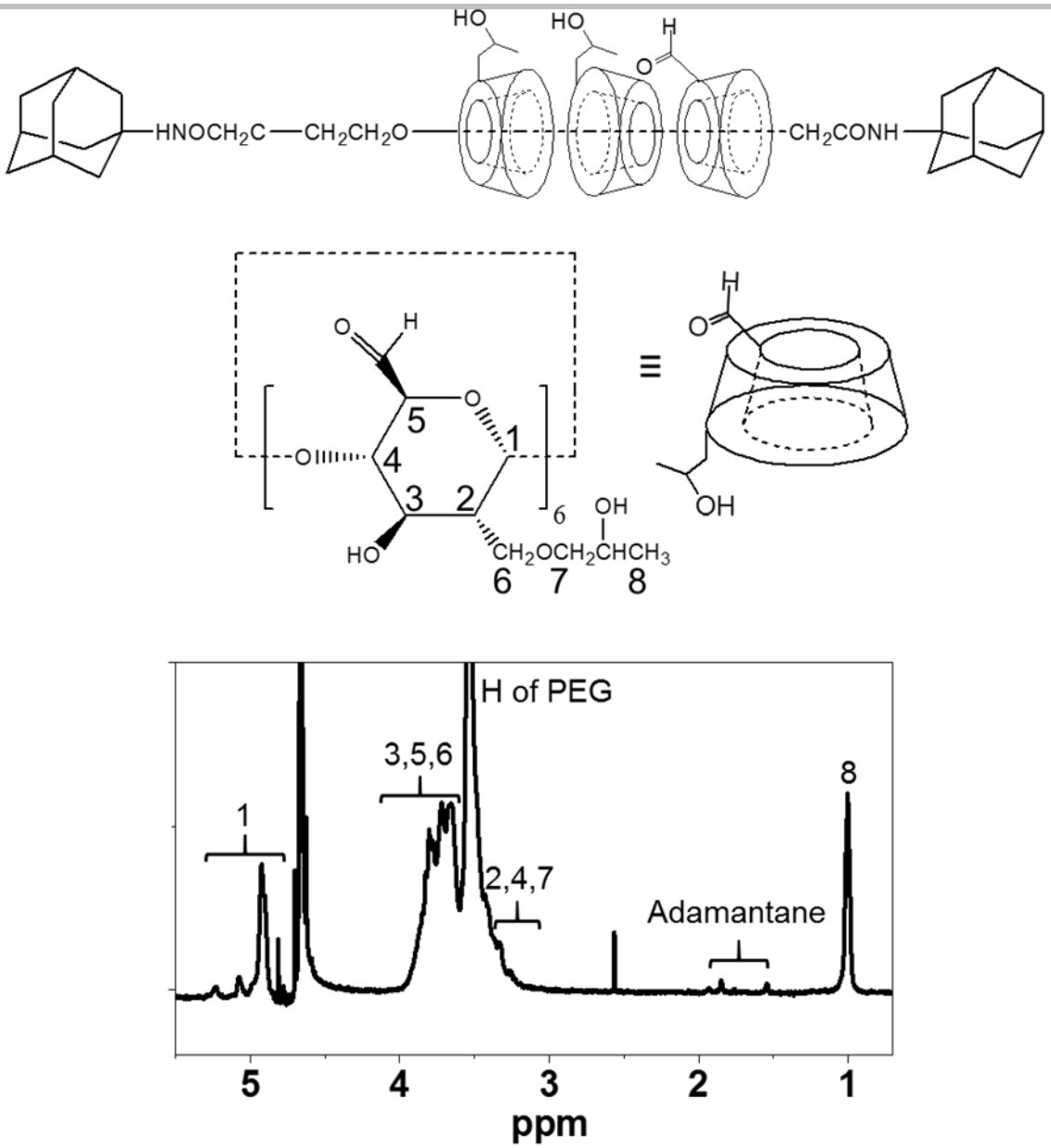

Figure S4. ^{1}H-NMR spectra of the hydroxylpropylated polyrotaxane aldehydes.

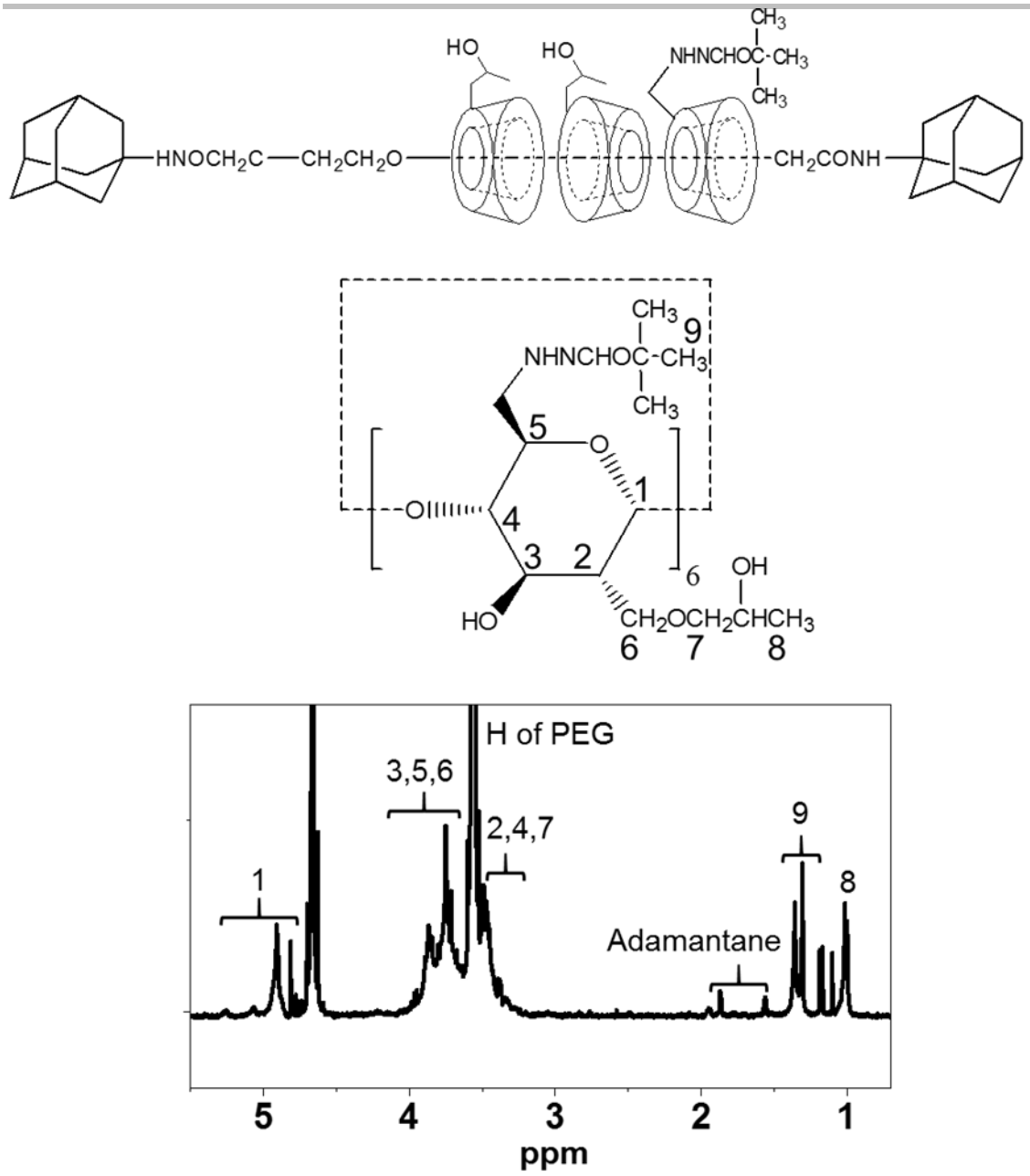

Figure S5. 1H-NMR spectra of the hydroxylpropylated polyrotaxane tert-butyl carbazate.

SUPPORTING INFORMATION

Table S1. Gelation time of HP-PRX-ALD/GC gel

Sample Code	Formulation		Gelation time (sec)
	Glycol chitosan (wt%)	HP-PRX$_X$-ALD (wt%)	
HP-PRX$_5$-ALD/GC	5.0	5.0	1383
HP-PRX$_{7.5}$-ALD/GC	5.0	7.5	258
HP-PRX$_{10}$-ALD/GC	5.0	10.0	165

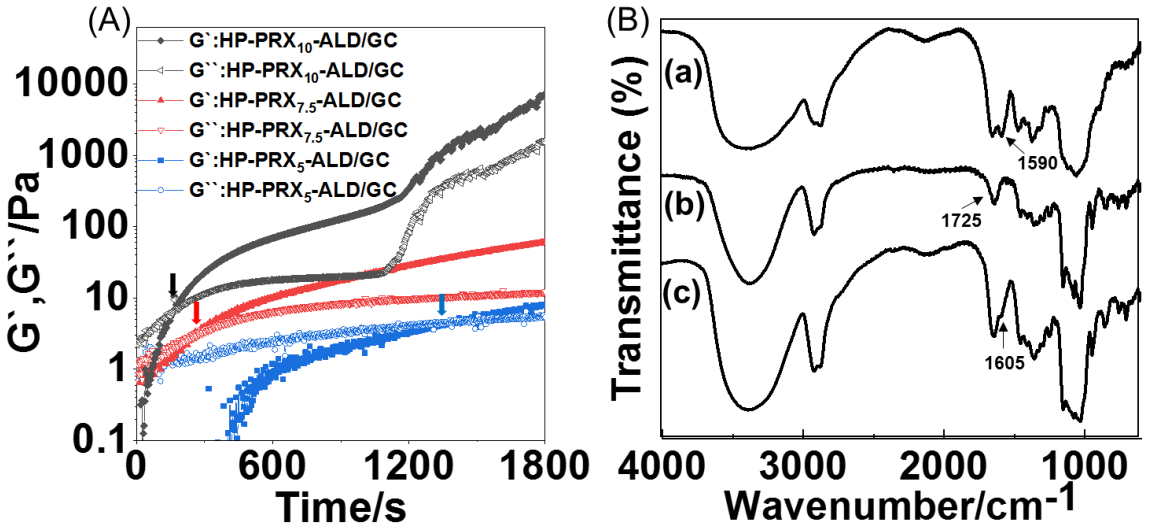

Figure S6. (A) Time evolution of storage modulus (G`) and loss modulus (G``) for HP-PRX-ALD/GC gel at 37 ºC. The time where G` and G`` crossover is denoted as gelation point (arrow). (B) FT-IR spectra of (a) GC, (b) HP-PRX-ALD, and (c) HP-PRX-ALD/GC gel.

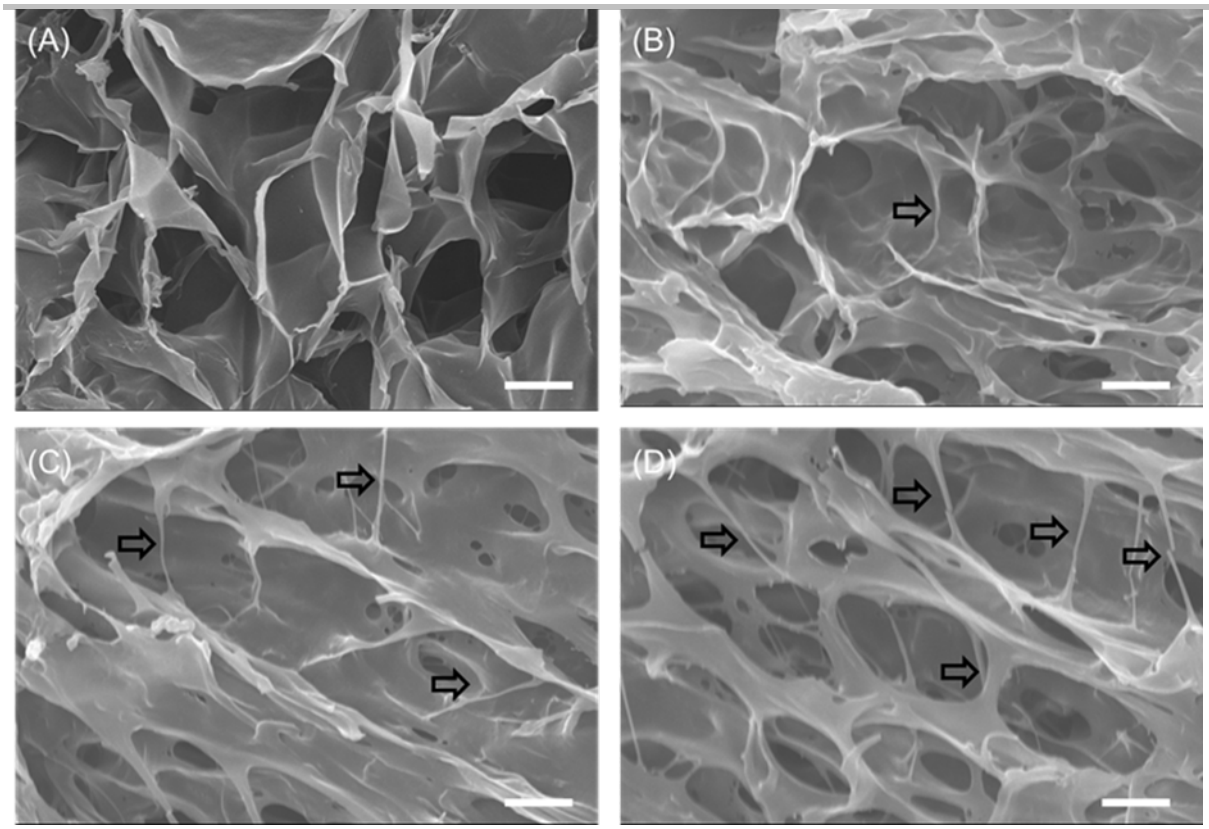

Figure S7. Cross-sectional SEM images of (A) Odex/GC hydrogel, (B) HP-PRX$_5$-ALD/GC, (C) HP-PRX$_{7.5}$-ALD/GC, (D) HP-PRX$_{10}$-ALD/GC. Fibrils are indicated by arrow. Scale bar 5 μm.

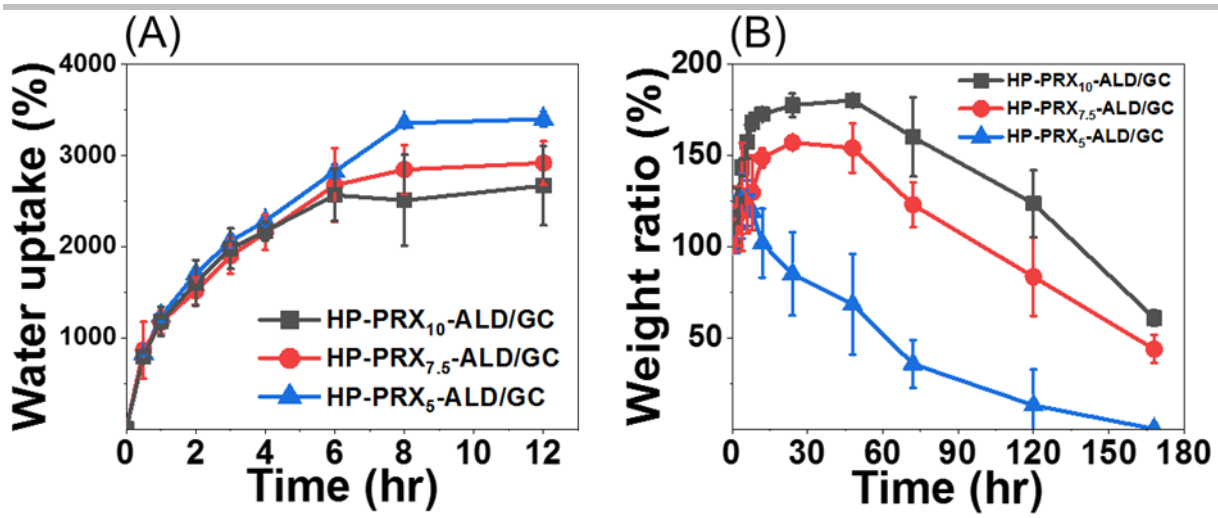

Figure S8. (A) Swelling ratio of the HP-PRX-ALD/GC gel with different HP-PRX-ALD concentration. (B) In vitro degradation of hydrogels in PBS at 37 °C as function of time.

Author Contributions

Conceptualization, T. Ooya; methodology, I. Cho and T. Ooya; investigation, I. Cho; writing—original draft preparation, I. Cho; writing—review and editing, T. Ooya; supervision, T. Ooya; project administration, T. Ooya; funding acquisition, I. Cho and T. Ooya.